

Dense bubble flow in a silo: a particular granular material

Y. Bertho, Ch. Becco, H. Caps & N. Vandewalle

Group for Research and Applications in Statistical Physics (GRASP)
Institut de Physique, Université de Liège, Belgium

ABSTRACT: The flow of air bubbles in a two-dimensional silo is studied experimentally. A particle tracking technique has been used to bring out the main properties of the flow: displacements of the bubbles, transverse and axial velocities. Air bubbles behave like solid grains in a granular flow. Correlations between the bubble velocities and their deformations have been observed.

1 INTRODUCTION

Structured fluids like granular materials and ordered foams received much attention from physicists this last decade. Indeed, these materials exhibit unusual rheological features as compared to conventional liquids. The particular case of dense granular flow is a complex phenomenon which involves multiple physical processes such as collisions and friction between the particles and with the channel walls (GdR-MiDi 2004). In order to drastically reduce both processes, we have experimentally investigated the rheology of dense monodisperse bubble flows. The flow of bubbles is of physical interest since contacting bubbles are characterized by a nearly zero friction: thus, we have a remarkable system with a low energy dissipation at the contacts. Even if bubble flows present strong analogies with granular flows, we must keep in mind that the nature of the interactions between the particles is totally different. Moreover, in contrast to granular materials, the bubbles may undergo strong deformations when they are subjected to a constraint. By comparing the flows of bubbles and granular media, significant physical properties are identified. This work presents a progress to understand and analyze the main flow characteristics in such dispersed media.

2 EXPERIMENTAL SETUP

Our experiment is analogous to the gravity-driven granular flow in a flat bottomed 2D silo, emptying out of a central orifice (Medina et al. 1998). In

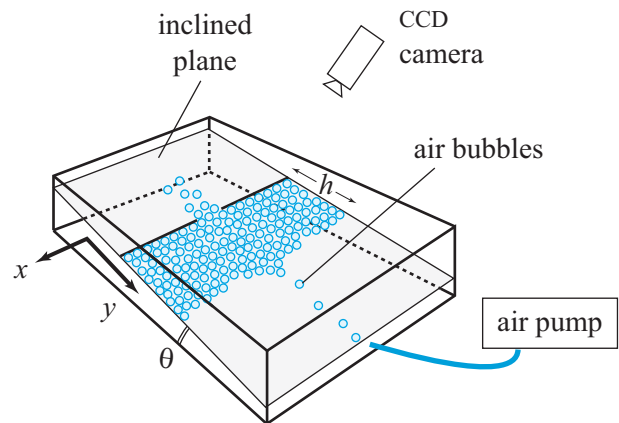


Figure 1. Sketch of the experimental setup. A transparent inclined plane is immersed into water and tilted at an angle θ . Small air bubbles are injected from below at the bottom of the plane and rise towards the top where they aggregate. Motions of the bubbles are recorded by a CCD camera.

1947, Bragg and coworkers proposed a simple experiment to put into evidence some crystallographic ordering (Bragg & Nye 1947; Feynman et al. 1964). It consisted in producing small identical bubbles at the surface of a liquid. Hexagonal packed structures appeared and crystallographic domains separated by grains boundaries were observed. We propose to modify Bragg's experiment to study dense flows of monodisperse bubbles (Vandewalle et al. 2004; Caps et al. 2004).

The experimental setup consists of a transparent inclined glass plane of width $W = 130$ mm which is immersed into water (Fig. 1). The tilt angle θ can be adjusted by a fine screwing system. Spherical monodis-

perse air bubbles are injected from below at the bottom of the inclined plane (the height h of the piling is kept roughly constant in the experiments $h \simeq 200$ mm). Note that the tilt angle is small (θ ranges from 0° to 1°) to ensure that only one layer of bubbles is created in the direction perpendicular to the plane. Bubble size can be controlled by an air pump and is kept roughly constant in the present study [diameter $d = (4.0 \pm 1.0)$ mm]. In order to avoid the coalescence of the bubbles, a small amount of surfactant is added into water. Due to buoyancy, the bubbles rise underneath the inclined plane and tend to pack on the transverse wall placed at the top of the plane. An orifice of width $D = (8.6 \pm 0.5)$ mm at the center (x_0, y_0) of this obstacle allows the bubbles to empty out the silo. Top views of the bubble packing are recorded through the transparent tilted plane by means of a CCD camera. Movies of the evolution of the packing are recorded at a frame rate of 30 frames per second. In order to quantify and to measure the main properties of the flow, each bubble of the packing (approximately 2000 bubbles per frame) has been tracked through image analysis.

3 EXPERIMENTAL RESULTS

3.1 Velocity profiles

Figure 2 displays the transverse v_x and longitudinal v_y velocities of the bubbles as a function of x and y . In the top part of the silo [(\blacktriangle) in Fig. 2b], a block motion is observed: the longitudinal velocity v_y remains constant reflecting low interactions between the bubbles and the side walls (slipping motion). As y decreases (*i.e.* the bubbles move towards the outlet), the flow takes place in a triangular-shaped domain where the fastest bubbles are located in the center of the silo and the slowest or motionless ones at the walls [(\blacktriangledown) in Fig. 2b]. This is in agreement with the V-shape of mobile grains observed during the flow of granular materials in silos or hourglasses (Hirshfeld et al. 1997; Medina et al. 1998; Samadani et al. 1999). Far from the outlet ($y \gtrsim 15d$), bubbles have a nearly zero transverse velocity (Fig. 2c) and a constant longitudinal velocity v_y (Fig. 2d). As y decreases the velocity distribution of the bubbles deep inside the silo is totally modified: a transverse component of velocity v_x appears in the flow conducting the bubbles towards the orifice while v_y increases strongly near the outlet.

3.2 Correlation velocity-deformation

Direct views of the dense bubble flow are recorded with a CCD camera and analyzed to extract the po-

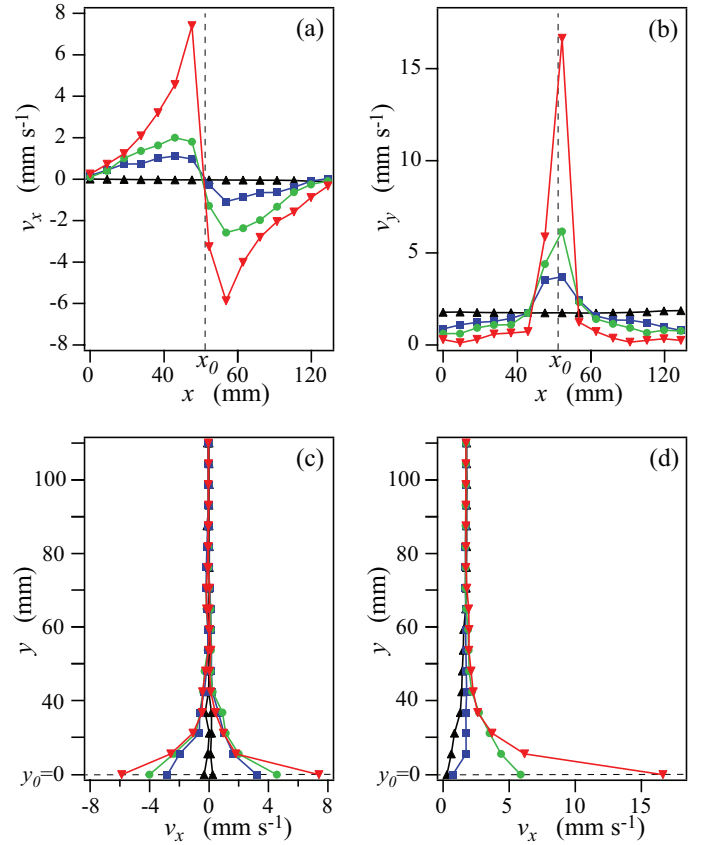


Figure 2. Transverse v_x and longitudinal v_y velocity profiles during a discharge of a silo ($\theta \simeq 0.6^\circ$). (—) position (x_0, y_0) of the center of the outlet of the silo. The different curves (\blacktriangledown , \bullet , \blacksquare , \blacktriangle) correspond respectively to velocity profiles at increasing distances from $y_0 = 0$ (Figs. 2a and 2b) and increasing distances from x_0 (Figs. 2c and 2d).

sition of each bubble in the stack. This allows computation of the displacement and the velocity of the bubbles during the flow. Moreover, the eccentricity of the bubbles is evaluated using image analysis and provides information concerning the constraints undergone inside the dense bubble assembly. A zoom of the bottom part of the silo of height 60 mm is shown in Fig. 3. The successive images correspond respectively to (a) a snapshot of the flow, (b) the displacement profiles of the bubbles, (c and d) the velocity field and the deformation field in the piling at the same instant during the flow.

As expected in two-dimensional nearly monodisperse flows, note that bubbles tend to pack in an ordered hexagonal structure at the top of the bubble piling. This organization is confirmed by plotting the distance between the bubbles and their first neighbours [(\blacktriangle) in Fig. 4]. Near the outlet of the silo, the bubbles undergo important constraints and tend to become more flat: this results in a decrease of the peaks of the correlation function G that appear at distances $l < d$ [(\blacktriangledown) in Fig. 4]. Note that the dashed lines in Fig. 4 represent the distance of the most neighbour-

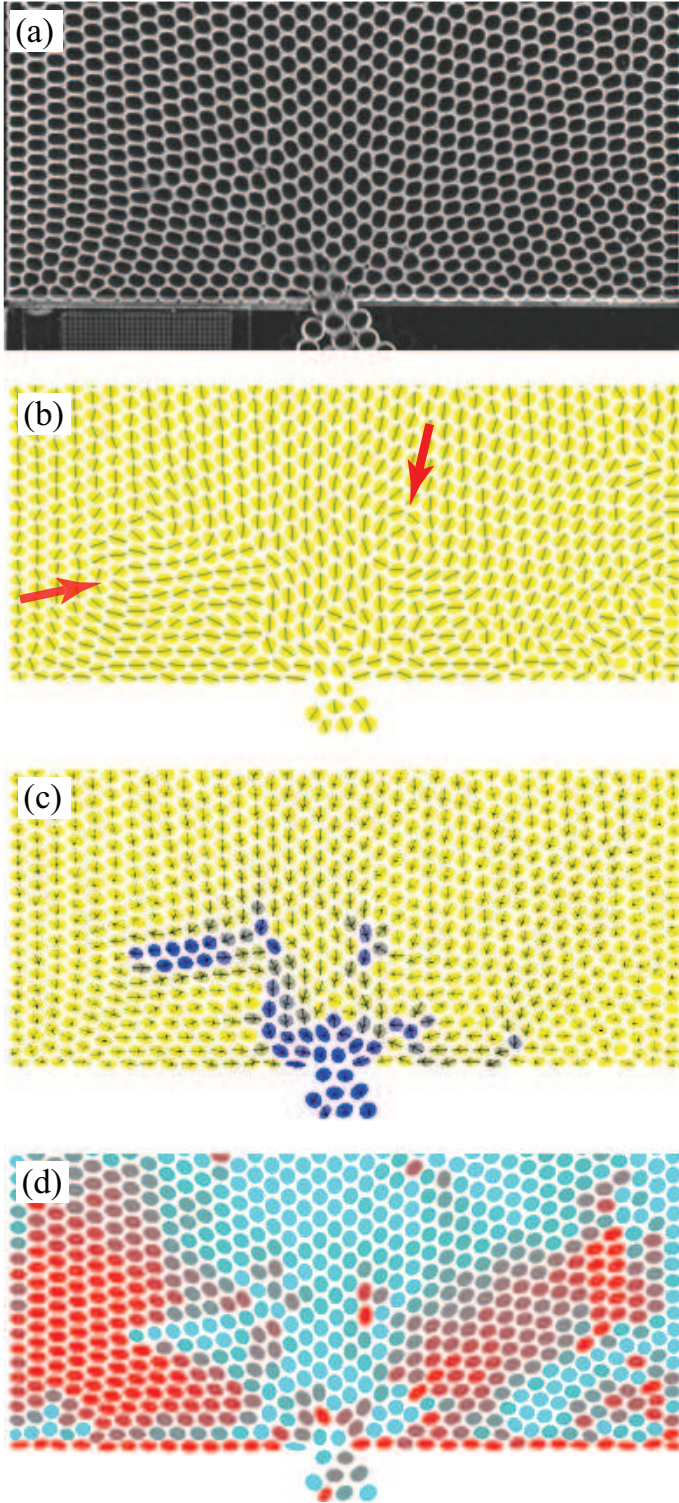


Figure 3. Typical recordings of the bubble discharge of the silo. From top to bottom: (a) snapshot of the experimental flow, (b) displacement field, (c) velocity field (the fastest bubbles appear darker), (d) deformation field (the more constrained bubbles appear darker).

ing bubbles in a perfect hexagonal lattice.

Figure 3b displays the displacement field of the bubbles during a discharge. In contrast with granular materials where the flow occurs only in a cone-shaped central region of the silo (while the grains lo-

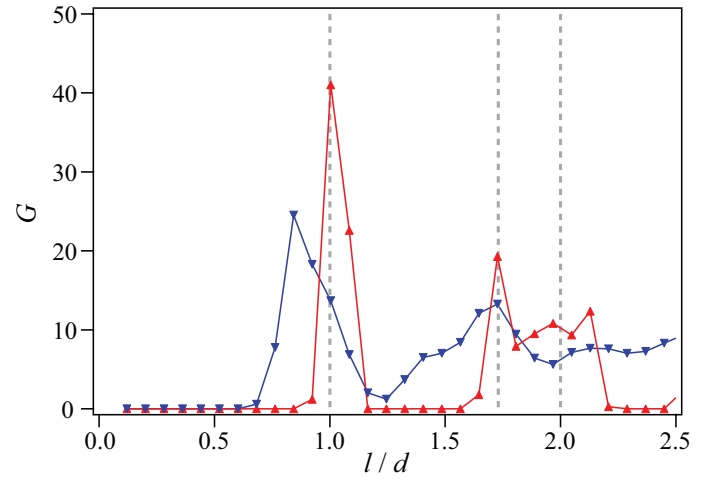


Figure 4. Correlation function G of the most neighbouring bubbles as a function of the distance l . The curves correspond to the number of neighbours in a 35×35 mm region, (▲) at the top of the bubble pile, (▼) near the outlet. Grey dashed lines correspond respectively to the distance between a particle and its first neighbours in a perfect hexagonal lattice.

cated in the regions near the side walls are motionless) (Medina et al. 1998; Samadani et al. 1999), note that motions of bubbles are detected in the whole silo. Moreover, the tracking put into evidence recirculation zones and the propagation of dislocations (shear bands) during the bubble flow. Motions of blocks of bubbles are observed and look like crystal domains. Those blocks are sliced by fast-moving defects (dislocations) along bubble lines. Both recirculation zone and dislocation appear clearly in Fig. 3b as pointed out by the arrows on the graph.

The velocity $v = \sqrt{v_x^2 + v_y^2}$ of each bubble has been computed and superimposed on the images of the flow (the darkest bubbles corresponding to the fastest ones). The recirculation regions and the dislocation observed in Fig. 3b are characterized by a mean velocity higher than in the rest of the silo (Fig. 3c).

The deformation of a bubble is evaluated by fitting the bubble shape by an ellipse and computing the eccentricity e given by:

$$e = \left(1 - \frac{b^2}{a^2}\right)^{1/2},$$

where a and b correspond respectively to the length of the major and minor axes of the ellipse. A correlation between the eccentricity of the bubbles and their velocity has been noticed. As pointed out in Fig. 3d, the fastest bubbles are observed to correspond to the less deformed ones. Moving bubbles tend to press against surrounding ones and deform them. This is especially the case near the dislocation. These observations are confirmed by plotting the velocity v of each bubble

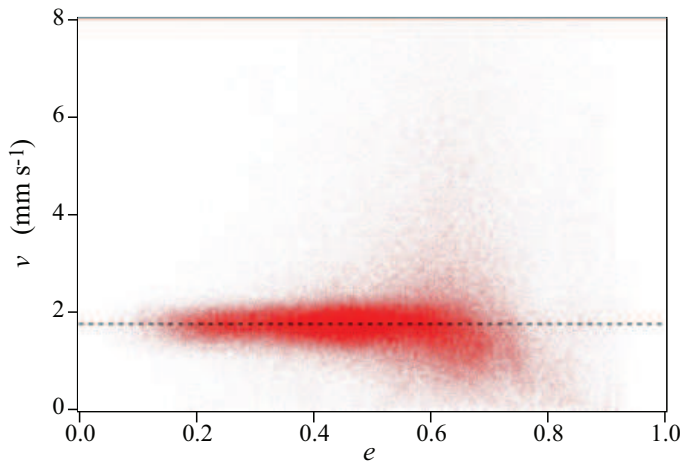


Figure 5. Velocity v of the bubbles as a function of their eccentricity e . Spherical bubbles are observed to move at a constant velocity while deformed ones correspond to the bubbles constrained near the walls or flowing out the silo.

as a function of their eccentricity e (Fig. 5). Therefore, in such dense bubble flows, spherical bubbles ($e \simeq 0$) are located far from the outlet and propagate in a block motion at a constant velocity, while flattest ones ($e \simeq 1$) correspond to crushed bubbles against the bottom wall or constraint bubbles inside the pile.

4" OUTLOOK

We have presented qualitative experimental results concerning the flow of dispersed media through a silo. Air bubbles have been used to simulate an ideal granular media since the friction between the bubbles is

nearly zero. Our study has pointed out similarities between granular and bubble flows: block motion far from the outlet, V-shape of velocity profiles,... A correlation between the deformation and the velocity of the bubbles has been found, where the slowest bubbles correspond to the more spherical ones and the fastest to the more deformed.

REFERENCES

- Bragg, W. L. & Nye, J. F. 1947. A dynamical model of a crystal structure. *Proc. R. Soc. London* 190: 474.
- Caps, H., Trabelsi, S., Dorbolo, S., & Vandewalle, N. 2004. Bubble and granular flows: differences and similarities. *Physica A* 344: 424.
- Feynman, R. P., Leighton, R. B., & Sands, M. 1964. *The Feynman lectures on physics* 2.
- GdR-MiDi 2004. On dense granular flows. *Eur. Phys. J. E* 14: 341.
- Hirshfeld, D., Radzyner, Y., & Rapaport, D. C. 1997. Molecular dynamics studies of granular flow through an aperture. *Phys. Rev. E* 56: 4404.
- Medina, A., Andrade, J., & Trevino, C. 1998. Experimental study of the tracer in the granular flow in a 2d silo. *Phys. Lett. A* 249: 63.
- Samadani, A., Pradhan, A., & Kudrolli, A. 1999. Size segregation of granular matter in silo discharges. *Phys. Rev. E* 60: 7203.
- Vandewalle, N., Trabelsi, S., & Caps, H. 2004. Block-to-granular-like transition in dense bubble flows. *Europhys. Lett.* 65: 316.